

Received 3 January 2019

Accepted 7 April 2019

Edited by B. D. Santarsiero, University of Illinois at Chicago, USA

**Keywords:** disaccharide; conformational analysis; crystal structure;  $\alpha$ -D-mannopyranosyl;  $\beta$ -D-mannopyranoside; glycobiology.

**CCDC reference:** 1908451

**Supporting information:** this article has supporting information at [journals.iucr.org/c](http://journals.iucr.org/c)

# Conformational analysis of the disaccharide methyl $\alpha$ -D-mannopyranosyl-(1 $\rightarrow$ 3)-2-O-acetyl- $\beta$ -D-mannopyranoside monohydrate

Wenhui Zhang, Qingquan Wu, Allen G. Oliver and Anthony S. Serianni\*

Department of Chemistry and Biochemistry, University of Notre Dame, Notre Dame, IN 46556-5670, USA.

\*Correspondence e-mail: aserianni@nd.edu

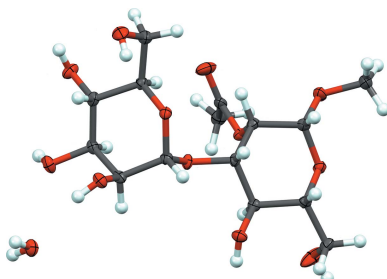
The crystal structure of methyl  $\alpha$ -D-mannopyranosyl-(1 $\rightarrow$ 3)-2-O-acetyl- $\beta$ -D-mannopyranoside monohydrate,  $C_{15}H_{26}O_{12}\cdot H_2O$ , (**II**), has been determined and the structural parameters for its constituent  $\alpha$ -D-mannopyranosyl residue compared with those for methyl  $\alpha$ -D-mannopyranoside. Mono-O-acetylation appears to promote the crystallization of (**II**), inferred from the difficulty in crystallizing methyl  $\alpha$ -D-mannopyranosyl-(1 $\rightarrow$ 3)- $\beta$ -D-mannopyranoside despite repeated attempts. The conformational properties of the O-acetyl side chain in (**II**) are similar to those observed in recent studies of peracetylated mannose-containing oligosaccharides, having a preferred geometry in which the C2—H2 bond eclipses the C=O bond of the acetyl group. The C2—O2 bond in (**II**) elongates by  $\sim$ 0.02 Å upon O-acetylation. The *phi* ( $\phi$ ) and *psi* ( $\psi$ ) torsion angles that dictate the conformation of the internal O-glycosidic linkage in (**II**) are similar to those determined recently in aqueous solution by NMR spectroscopy for unacetylated (**II**) using the statistical program *MA'AT*, with a greater disparity found for  $\psi$  ( $\Delta = \sim$ 16°) than for  $\phi$  ( $\Delta = \sim$ 6°).

## 1. Introduction

High-mannose N-glycans are important appendages that are covalently attached to proteins during translation *in vivo* and that derive from a common  $Glc_3Man_9GlcNAc_2$  precursor, (**I**) (Helenius & Aebi, 2001; Breitling & Aebi, 2013; Fig. 1). The biological functions of the glycan chains of high-mannose glycoproteins have been the subject of considerable study (Nagae & Yamaguchi, 2012; Satoh *et al.*, 2015). Elucidating the conformational properties of high-mannose oligosaccharides, either free in solution or bound to protein, remains an important goal in structural glycobiology, underpinned by the expectation that their conformational equilibria and dynamics influence their chemical and biochemical properties.

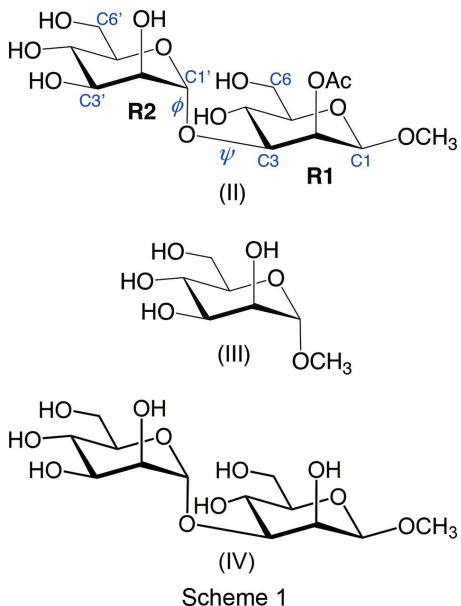
Inspection of the structure of (**I**) (Fig. 1) reveals the presence of two types of  $\alpha$ Man-(1 $\rightarrow$ 3)-Man O-glycosidic linkages, distinguished by the anomeric configuration of the Man residue that serves as an acceptor. In disaccharides, this difference appears to have little effect on linkage conformation, as shown recently in NMR studies using *MA'AT* analysis (Zhang *et al.*, 2017). In a larger oligosaccharide like (**I**), however, this difference may affect linkage geometry because of potentially different distributions and strengths of noncovalent interactions brought about by the different anomeric configurations.

Present work in this laboratory aims to improve current understanding of the conformational properties of large biologically important oligosaccharides like (**I**). The approach involves defining O-glycosidic linkage behaviors free of



© 2019 International Union of Crystallography

structural context (*i.e.* isolated linkages such as those found in disaccharides) in order to identify when these behaviors are perturbed in larger structures and, importantly, what structural factors are responsible for the perturbations. Crystallographic studies of isolated *O*-glycosidic linkages are also of value for direct comparison to the same linkages in solution to document the effects of solvation by explicit solvent molecules in solution and by solute–solute nonbonded interactions in the crystal lattice.



Scheme 1

Herein we report the crystal structure of the disaccharide methyl  $\alpha$ -D-mannopyranosyl-(1 $\rightarrow$ 3)-2-*O*-acetyl- $\beta$ -D-mannopyranoside monohydrate, (**II**), which contains an internal *O*-glycosidic linkage structurally related to that between residues 3 and 4 in (**I**). The comparison, however, is not a faithful one because of the 2-*O*-acetyl side chain present in the  $\beta$ Man residue of (**II**). This side chain was installed to promote crystallization; in its absence, the disaccharide was resistant to crystallization. Limited acylation may prove to be generally useful in efforts to crystallize other biologically important di- and oligosaccharides that have been refractory to crystallization in their fully deprotected forms.

## 2. Experimental

### 2.1. Synthesis and crystallization of (**II**) (see Fig. 2)

**2.1.1. Preparation of 2,3,4,6-tetra-*O*-acetyl- $\alpha$ -D-mannopyranosyl trichloroacetimidate, (**4**).** D-Mannose (**1**) (2.30 g, 12.78 mmol) was dissolved in pyridine (40 ml) and  $\text{Ac}_2\text{O}$  (10 ml, 105.8 mmol) was added. After stirring at room temperature for 12 h, the mixture was concentrated at 30 °C *in vacuo*. The residue was dissolved in  $\text{CHCl}_3$ , washed with water, dried over anhydrous  $\text{Na}_2\text{SO}_4$ , and concentrated to give **2**.

Compound **2** (1.95 g, 5.00 mmol) was dissolved in tetrahydrofuran (THF, 20 ml), the resulting solution was cooled in an ice bath, and  $\text{PhCH}_2\text{NH}_2$  (0.60 ml, 5.50 mmol) was added. After stirring for 4 h at room temperature, the THF was removed under vacuum and product **3** was purified by flash chromatography on silica gel (eluent = hexane/ethyl acetate, 1.5:1 *v/v*). A mixture of **3** (1.56 g, 4.48 mmol), trichloroacetonitrile (2.24 ml, 22.4 mmol), and several drops of 1,8-diazabicyclo[5.4.0]undec-7-ene (DBU) was added to  $\text{CH}_2\text{Cl}_2$  (30 ml), and the resulting solution was incubated at room temperature for 3 h and then concentrated *in vacuo*. Flash chromatography on silica gel (eluent = hexane/ethyl acetate, 2:1 *v/v*) gave trichloroacetimidate **4** (1.66 g, 3.38 mmol, 76%) (Schmidt & Michel, 1985).

**2.1.2. Preparation of methyl 4,6-*O*-benzylidene- $\beta$ -D-mannopyranoside, (**6**).** Methyl  $\beta$ -D-mannopyranoside (**5**) (1.32 g, 6.80 mmol) was stirred at room temperature in dry *N,N*-dimethylformamide (DMF) (30 ml) containing benzaldehyde dimethyl acetal (1.10 ml, 7.40 mmol) and a catalytic amount of *p*-toluenesulfonic acid (*p*-TsOH) for 2 d. The reaction mixture was neutralized by adding several drops of triethylamine. The mixture was evaporated to dryness *in vacuo* and purified by flash chromatography on silica gel (first eluent = hexane/ethyl acetate, 1:2 *v/v*; second eluent = methanol/ethyl acetate, 1:2 *v/v*), affording methyl glycoside **6** (1.23 g, 4.42 mmol, 65%) (Evans, 1980).

**2.1.3. Preparation of methyl 2,3,4,6-tetra-*O*-acetyl- $\alpha$ -D-mannopyranosyl-(1 $\rightarrow$ 3)-4,6-*O*-benzylidene- $\beta$ -D-mannopyranoside, (**7**).** Anhydrous  $\text{CH}_2\text{Cl}_2$  (40 ml) was added to a mixture of trichloroacetimidate **4** (700 mg, 1.42 mmol), methyl glyco-

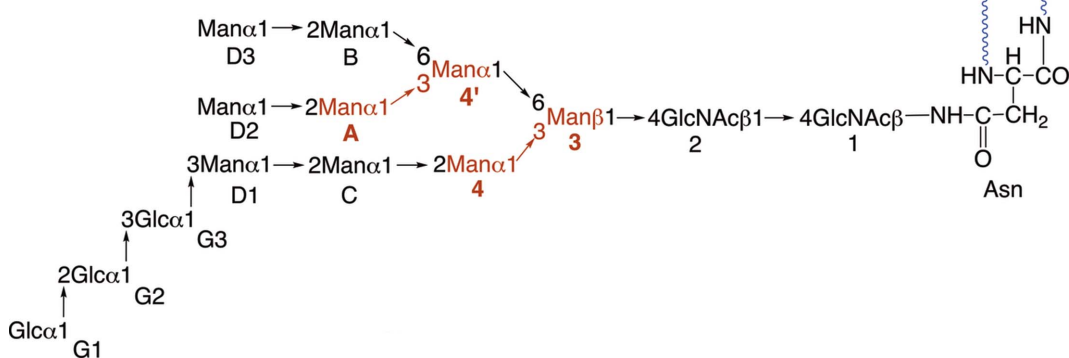


Figure 1  
The N-glycan precursor  $\text{Man}_9\text{GlcNAc}_2\text{Glc}_3$ , (**I**).

side **6** (440 mg, 1.55 mmol), and molecular sieves (4 Å, 2.0 g), which were dried under high vacuum. The solution was cooled to  $-78^{\circ}\text{C}$  and treated with a small amount of trimethylsilyl trifluoromethanesulfonate (TMSOTf) (20 µl, 0.11 mmol) under  $\text{N}_2$ . After 4 h, the reaction mixture was quenched with the addition of triethylamine and the molecular sieves were removed by filtration. The solution was concentrated *in vacuo* to a syrup, which was purified by flash chromatography on silica gel (eluant = hexane/ethyl acetate, 1:1 *v/v*) to afford disaccharide **7** (570 mg, 0.93 mmol, 66%) (Carpenter & Nepogodiev, 2005).

**2.1.4. Preparation of methyl 2,3,4,6-tetra-O-acetyl- $\alpha$ -D-mannopyranosyl-(1 $\rightarrow$ 3)-2-O-acetyl-4,6-O-benzylidene- $\beta$ -D-mannopyranoside, (8).** Disaccharide **7** (200 mg, 0.33 mmol) was dissolved in pyridine (10 ml) and  $\text{Ac}_2\text{O}$  (0.10 ml, 1.06 mmol) was added. After stirring at room temperature for 12 h, the mixture was concentrated at  $30^{\circ}\text{C}$  *in vacuo*. The residue was dissolved in  $\text{CHCl}_3$ , washed with water, dried over anhydrous  $\text{Na}_2\text{SO}_4$ , and concentrated to give compound **8** (210 mg, 0.32 mmol, 98%).

**2.1.5. Preparation of methyl 2,3,4,6-tetra-O-acetyl- $\alpha$ -D-mannopyranosyl-(1 $\rightarrow$ 3)-2-O-acetyl- $\beta$ -D-mannopyranoside, (9).** Compound **8** (200 mg, 0.31 mmol) was dissolved in methanol (20 ml) and acetyl chloride (20 µl) was added at  $0^{\circ}\text{C}$ . The reaction mixture was stirred for 2 h and then neutralized with the addition of a few drops of trimethylamine. The solution was concentrated *in vacuo* to a syrup, which was purified by flash chromatography on silica gel (eluant = ethyl acetate) to afford **9** (147 mg, 0.26 mmol, 85%).

**2.1.6. Preparation of methyl  $\alpha$ -D-mannopyranosyl-(1 $\rightarrow$ 3)-2-O-acetyl- $\beta$ -D-mannopyranoside, (II).** Compound **9** (147 mg, 0.26 mmol) was dissolved in methanol (10 ml) and sodium methoxide was added until the pH of the solution reached 10. The reaction mixture was stirred for 0.5 h at room temperature and then neutralized with Dowex 50 ion-exchange resin in the  $\text{H}^+$  form. After the resin had been removed by filtration, the filtrate was concentrated *in vacuo* to a syrup and purified by flash chromatography on silica gel (eluant =  $\text{CH}_2\text{Cl}_2$ /

**Table 1**  
Experimental details.

Crystal data	$\text{C}_{15}\text{H}_{26}\text{O}_{12}\cdot\text{H}_2\text{O}$
Chemical formula	$\text{C}_{15}\text{H}_{26}\text{O}_{12}\cdot\text{H}_2\text{O}$
$M_r$	416.37
Crystal system, space group	Hexagonal, $P6_5$
Temperature (K)	120
$a, c$ (Å)	7.8682 (3), 52.555 (3)
$V$ (Å $^3$ )	2817.7 (3)
$Z$	6
Radiation type	$\text{Cu K}\alpha$
$\mu$ (mm $^{-1}$ )	1.13
Crystal size (mm)	0.30 $\times$ 0.23 $\times$ 0.14
Data collection	
Diffractometer	Bruker APEXII
Absorption correction	Numerical ( <i>SADABS</i> ; Krause <i>et al.</i> , 2015)
$T_{\min}, T_{\max}$	0.816, 0.907
No. of measured, independent and observed [ $I > 2\sigma(I)$ ] reflections	37134, 3719, 3719
$R_{\text{int}}$	0.021
(sin $\theta/\lambda$ ) $_{\text{max}}$ (Å $^{-1}$ )	0.619
Refinement	
$R[F^2 > 2\sigma(F^2)]$ , $wR(F^2)$ , $S$	0.022, 0.058, 1.06
No. of reflections	3719
No. of parameters	287
No. of restraints	1
H-atom treatment	H atoms treated by a mixture of independent and constrained refinement
$\Delta\rho_{\text{max}}, \Delta\rho_{\text{min}}$ (e Å $^{-3}$ )	0.20, -0.16
Absolute structure	Flack $x$ determined using 1835 quotients $[(I^+) - (I^-)]/[(I^+) + (I^-)]$ (Parsons <i>et al.</i> , 2013)
Absolute structure parameter	0.028 (14)

Computer programs: *APEX3* (Bruker, 2015), *SAINT* (Bruker, 2015), *SHELXT2014* (Sheldrick, 2015a), *SHELXL2018* (Sheldrick, 2015b), *Mercury* (Macrae *et al.*, 2008), *publCIF* (Westrip, 2010) and *PLATON* (Spek, 2009).

methanol, 2:1 *v/v*), affording product (**II**) (yield 41 mg, 0.10 mmol, 38%). A secondary product, namely methyl  $\alpha$ -D-mannopyranosyl-(1 $\rightarrow$ 3)- $\beta$ -D-mannopyranoside, (**IV**) (yield 47 mg, 0.13 mmol, 50%), was also isolated in pure form. A table of  $^1\text{H}$  and  $^{13}\text{C}$  NMR chemical shifts for (**II**) is available in

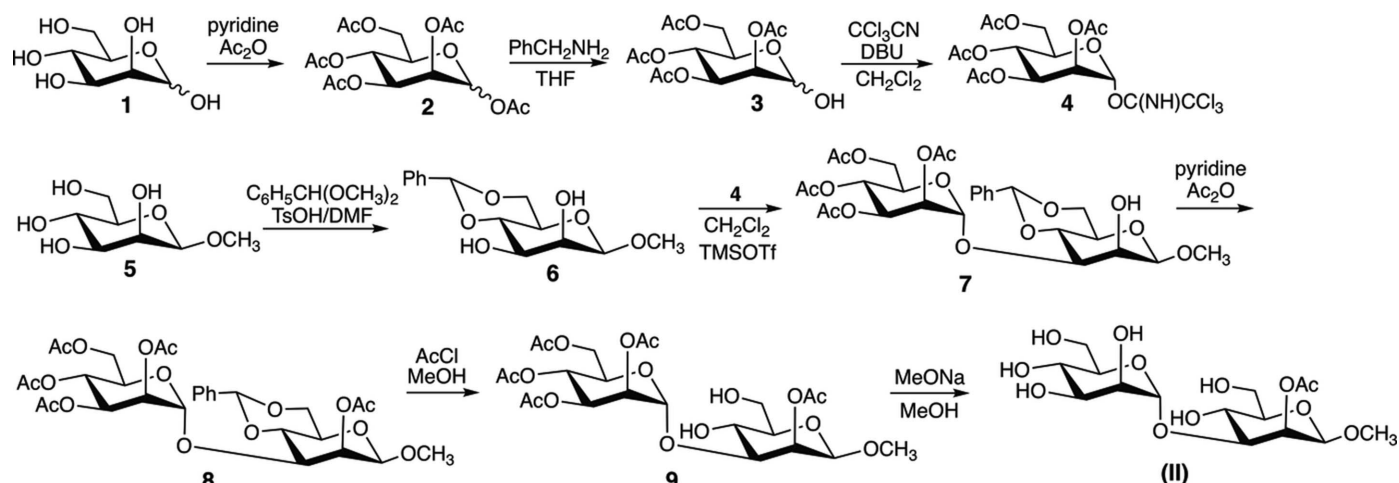


**Figure 2**  
The synthetic pathway for the preparation of (**II**).

the supporting information. Disaccharide (**II**) was dissolved in a minimum quantity of distilled water and the solution was stored at 4 °C until crystals formed.

## 2.2. Refinement

Crystal data, data collection and structure refinement details are summarized in Table 1. H atoms bonded to carbon were refined in geometrically calculated positions, with C—H = 1.00 (methine), 0.99 (methylene), and 0.98 Å (methyl), and with  $U_{\text{iso}}(\text{H}) = 1.2U_{\text{eq}}(\text{C})$  (methine and methylene) or  $1.5U_{\text{eq}}(\text{C})$  (methyl). Hydroxy and water H atoms were located from a difference Fourier map and freely refined.

## 3. Results and discussion

Compound (**II**) crystallizes as the monohydrate in the chiral hexagonal space group  $P6_5$  (Fig. 3). Bond distances and angles within the molecule are as expected. A summary of the structural parameters for (**II**) and methyl  $\alpha$ -D-mannopyranoside, (**III**) (Jeffrey *et al.*, 1977), is provided in Table 2. Structural comparisons between the R2 residue of (**II**) and (**III**) are made in this report, but those between the R1 residue of (**II**) and either methyl 2-O-acetyl- $\beta$ -D-mannopyranoside or methyl  $\beta$ -D-mannopyranoside cannot be made because crystal structures of the latter are not currently available.

The average exocyclic C5—C6 bond length in both residues of (**II**) [1.513 (6) Å] is shorter than the remaining endocyclic C—C bond lengths [1.525 (6) Å]. The C1—O1 bond in the  $\beta$ Man residue (R1) of (**II**) appears to be shorter than that observed in the  $\alpha$ Man residue (R2), and the latter length is similar to the C1—O1 bond length in (**III**). However, the endocyclic C1—O5 bonds in R1 and R2 of (**II**) are very similar in length, suggesting that differential lone-pair donation into this bond in these residues, perhaps due to the different anomeric configurations, cannot explain the difference in the C1—O1 bond length. The latter difference may be explained by bond orientation (axial bonds are often longer than equatorial bonds regardless of their location in pyranosyl

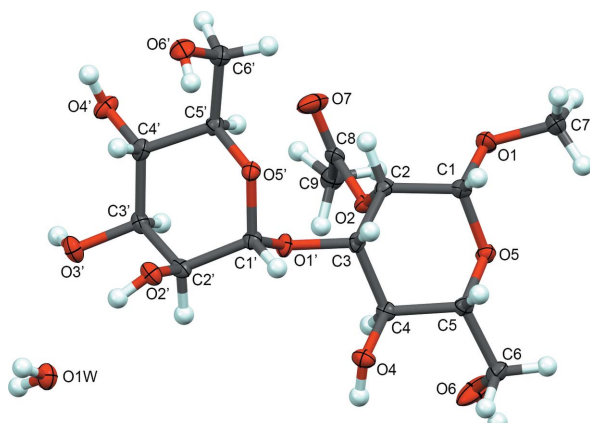


Figure 3

Labeling scheme for disaccharide (**II**). Displacement ellipsoids are depicted at the 50% probability level and H atoms are shown as spheres of arbitrary radius.

Table 2

Selected bond lengths, bond angles, and torsion angles in methyl  $\alpha$ -D-mannopyranosyl-(1→3)-2-O-acetyl- $\beta$ -D-mannopyranoside monohydrate, (**II**), and methyl  $\alpha$ -D-mannopyranoside, (**III**).

Structural parameter	Compound/residue		
	( <b>II</b> ) (R1) <sup>a</sup>	( <b>II</b> ) (R2) <sup>d</sup>	( <b>III</b> ) <sup>c</sup>
Bond lengths (Å)			
C1—C2	1.524 (2)	1.525 (2)	1.524
C2—C3	1.520 (2)	1.521 (2)	1.529
C3—C4	1.520 (2)	1.524 (2)	1.519
C4—C5	1.537 (2)	1.531 (2)	1.529
C5—C6	1.508 (2)	1.517 (2)	1.518
C1—O1	1.383 (2)	1.407 (2)	1.400
C1—O5	1.426 (2)	1.422 (2)	1.415
C2—O2	1.444 (2)	1.429 (2)	1.415
C3—O1'	1.429 (2)		
C3—O3		1.417 (2)	1.422
C4—O4	1.428 (2)	1.428 (2)	1.430
C5—O5	1.435 (2)	1.452 (2)	1.435
C6—O6	1.417 (2)	1.419 (2)	1.413
O1—CH <sub>3</sub>	1.437 (2)		1.423
Bond angles (°)			
C5—O5—C1	111.68 (12)		
C5'—O5'—C1'	114.20 (12)		114.29
C1'—O1'—C3	113.60 (13)		
C1—O1—CH <sub>3</sub>	113.08 (14)		113.91
C2—O2—C <sub>car</sub> <sup>b</sup>	119.09 (13)		
O2—C <sub>car</sub> —C <sub>Me</sub>	110.13 (15)		
O2—C <sub>car</sub> —O <sub>car</sub>	123.98 (18)		
O <sub>car</sub> —C <sub>car</sub> —C <sub>Me</sub>	125.89 (17)		
Bond torsions (°)			
C1—C2—C3—C4	−55.19 (17)		
C1—O5—C5—C4	62.30 (17)		
C1'—C2'—C3'—C4'	−54.41 (18)		−53.37
C1'—O5'—C5'—C4'	58.19 (17)		59.13
C2—C1—O1—CH <sub>3</sub> (φ)	161.85 (15)		
O5—C1—O1—CH <sub>3</sub> (φ)	−79.07 (18)		
H1—C1—O1—CH <sub>3</sub> (φ)	40.93		
C2'—C1'—O1'—C3 (φ')	−160.26 (13)		−177.69
O5'—C1'—O1'—C3 (φ')	77.51 (16)		60.51
H1'—C1'—O1'—C3 (φ')	−42.68		−56.22
C1'—O1'—C3—C2 (ψ')	−125.72 (15)		
C1'—O1'—C3—C4 (ψ')	112.14 (14)		
C1'—O1'—C3—H3 (ψ')	−6.43		
O5—C5—C6—O6	−63.86 (19) (gg)		
O5'—C5'—C6'—O6'	−69.90 (18) (gg)		−65.10 (gg)
C1—C2—O2—C <sub>car</sub>	−114.09 (16)		
H2—C2—O2—C <sub>car</sub>	6.63		
C3—C2—O2—C <sub>car</sub>	128.63 (15)		
C2—O2—C <sub>car</sub> —C <sub>Me</sub>	168.49 (15)		
C2—O2—C <sub>car</sub> —O <sub>car</sub>	−11.7 (3)		

Notes: (a) R1 and R2 denote the  $\beta$ Man and  $\alpha$ Man residues in disaccharide (**II**), respectively; see structure in text. (b) C<sub>car</sub> is the carbonyl C atom of the 2-O-acetyl side chain of (**II**), O<sub>car</sub> is the carbonyl O atom of the side chain, and C<sub>Me</sub> is the methyl C atom of the side chain. (c) Bond angles and torsions in (**III**) are listed in some cases with primed atoms to allow visual comparison with the  $\alpha$ Man residue (R2) of (**II**); data were taken from Jeffrey *et al.* (1977). (d) Bonds are shown with unprimed atoms in residue R2 of (**II**) to simplify structural comparisons in the table. gg = gauche-gauche.

rings) and/or differential effects of the axial O2 atom on the C1—O1 bond length (e.g. the antiperiplanar O1'—O2' arrangement in R2 leads to C1'—O1' bond elongation). The noticeably longer C2—O2 bond in R1 relative to R2 is caused mainly by the O-acetyl side chain, which is known to lengthen the ester C—O bond by ~0.02 Å relative to the same bond when the OH group is unprotected (Turney *et al.*, 2019). However, comparisons of corresponding C—O bond lengths in R2 of (**II**) and (**III**) are not straightforward because the

Table 3

Cremer–Pople puckering parameters for aldohexopyranosyl residues in (II) and (III).

Compound/residue	$\theta$ (°)	$\varphi$ (°)	$Q$ (Å)	$q_2$ (Å)	$q_3$ (Å)
(II): $\beta$ Man (R1)	2.00 (18)	16 (5)	0.5893 (18)	0.0208 (18)	0.5889 (18)
(II): $\alpha$ Man (R2)	2.78 (18)	230 (2)	0.5659 (18)	0.0303 (18)	0.5653 (18)
(III): $\alpha$ Man <sup>a</sup>	1.2	286	0.557	0.0118	0.5569

Note: (a) errors were not reported for structure (III); data were taken from Jeffrey *et al.* (1977).

hydrogen-bonding behaviors of these rings in the crystals are not identical (see below); hydrogen bonding will affect these bond lengths depending on whether the OH group is participating as a donor, an acceptor, or both (Hadad *et al.*, 2017).

The endocyclic C1–O5–C5 bond angle in R1 is smaller than that in R2, with the latter matching that found in (III) (Table 2). Likewise, the C1–O1–CH<sub>3</sub> bond angles in R1 of (II) and (III) are similar despite the difference in the anomeric configurations. While the angle in (III) compares favorably with the C1'–O1'–C3 *O*-glycosidic bond angle in (II), the different anomeric configurations of the two linkages combined with the different aglycone groups prevents a meaningful comparison.

The structural parameters associated with the *O*-acetyl side chain appended to R1 of (II) resemble those found in prior crystal structures of *O*-acetylated  $\alpha$ -D-mannopyranosyl rings (Turney *et al.*, 2019). Specifically, the H2–C2–O2–C<sub>car</sub> and C2–O2–C<sub>car</sub>–O<sub>car</sub> torsion angles are close to 0°, causing the C2–H2 and C<sub>car</sub>–O<sub>car</sub> bonds to be nearly eclipsed (Table 2; C<sub>car</sub> = C8, O<sub>car</sub> = O7, and C<sub>Me</sub> = C9). Bond angles involving C<sub>car</sub> of the side chain are not equivalent, with the O2–C<sub>car</sub>–C<sub>Me</sub> bond angle significantly smaller than the remaining two bond angles, as observed in related systems (Turney *et al.*, 2019). Other torsion angles that R2 of (II) and (III) have in common show similar properties. For example, the C2–C1–O1–C<sub>aglycone</sub> torsion angles are similar (−160 and −178°, respectively), with the latter approaching an ideal anti-periplanar geometry, as expected from the *exo*-anomeric effect (Thøgersen *et al.*, 1982; Kirby, 1983; Tvaroška & Bleha,

1989; Alabugin, 2016), and which presumably is reduced in the internal glycoside linkage in (II) due to structural constraints imposed by the bulkier aglycone.

Both Man residues of (II) and (III) contain exocyclic hydroxymethyl (−CH<sub>2</sub>OH) groups in the *gauche–gauche* (gg) conformation, that is, with C6 roughly antiperiplanar to H5 (Table 3).

Cremer–Pople values for the two  $\alpha$ -D-mannopyranosyl rings in (II) and in (III) are given in Table 3. These rings show similar minor deviations from idealized  $^4C_1$  chair conformations, as indicated by the small values of  $\theta$  (1–3°). The directions of distortion are similar for the  $\alpha$ Man residue (R2) in (II) and that in (III) (towards  $^{1,4}B^1S_5$ ), but differ somewhat from that found for the  $\beta$ Man residue (R1) in (II) (towards  $^{3,0}B^3S_1$ ).

Recent NMR studies (Zhang *et al.*, 2019) using *MA'AT* analysis indicate that methyl  $\alpha$ -D-mannopyranosyl-(1→3)- $\beta$ -D-mannopyranoside, (IV), which is devoid of the *O*-acetyl group at C2 of (II), adopts a linkage conformation in aqueous solution similar to that found in crystalline (II). For (IV), mean values of the H1'–C1'–O1'–C3 ( $\varphi$ ) and C1'–O1'–C3–H3 ( $\psi$ ) torsion angles of −37 and 10°, respectively, were found in solution, while the crystal structure of (II) gives corresponding values of −43 and −6° (Table 2). In this case, lattice forces do not favor a linkage geometry appreciably different from that found in solution, unlike other cases where these perturbations can be significant, especially for the *psi* ( $\psi$ ) torsion angle (Zhang *et al.*, 2017).

No intra-residue hydrogen bonds are observed in the crystal structure of (II), but multiple hydrogen bonds exist between different molecules of (II) in the crystal lattice (Fig. 4 and Table 4). The glycosidic atoms O1 and O1' (the latter involved in the internal *O*-glycosidic linkage) do not participate in hydrogen bonding. In the  $\beta$ Man residue (R1) of (II), O2 does not participate in hydrogen bonding, whereas hydroxy groups O4 and O6 serve as donors and single hydrogen-bond acceptors. The ring oxygen (O5) and carbonyl oxygen (O7) of the 2-*O*-acetyl group in the  $\beta$ Man residue both serve as mono-acceptors. In the  $\alpha$ Man residue (R2) of (II), O2' serves as a

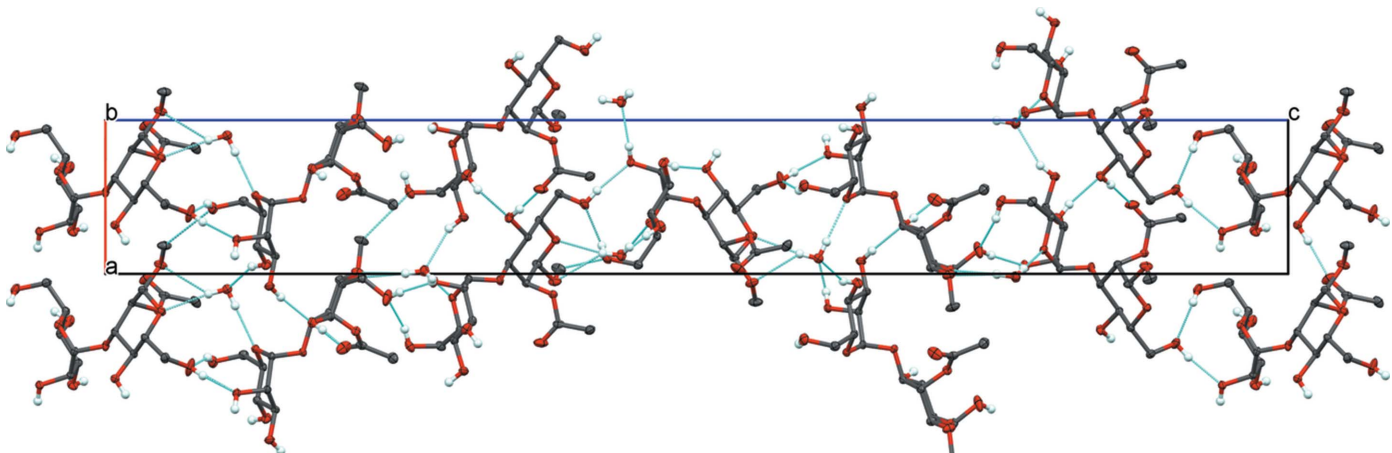


Figure 4

Packing diagram for (II) viewed along the  $b$  axis. H atoms not involved in hydrogen bonding have been omitted for clarity.

hydrogen-bond donor to the lattice water molecule and as a single hydrogen-bond acceptor, while hydroxy groups O3', O4', and O6' serve only as hydrogen-bond donors. The ring oxygen (O5') in the  $\alpha$ Man residue serves as a single hydrogen-bond acceptor. The lattice hydrogen-bonding pattern observed for monomer (**III**) differs somewhat from that observed in the  $\alpha$ Man residue (R2) of (**II**) in that both O1 and O5 serve as single hydrogen-bond acceptors, O2 and O6 serve as hydrogen-bond donors only, and O3 and O4 serve as hydrogen-bond donors and single hydrogen-bond acceptors.

Propagation along the *c* axis is through hydrogen bonds from O6'...O6<sup>v</sup> and O6<sup>v</sup>...O2' (see Table 4 for details and symmetry codes), related by the 6<sub>5</sub> screw axis (O6' and O2' are atoms in the reference molecule; Fig. 4). This chain of molecules links to other chains via O3'...O4<sup>iii</sup> and O4...O7<sup>i</sup> hydrogen bonds. The water of crystallization (O1W) is also involved in interchain hydrogen bonding, serving as an acceptor for hydrogen bonds from O2' and O4' (O2'...O1W and O4'...O1W<sup>iv</sup>). O1W is a hydrogen-bond donor to anomeric atoms O5<sup>vi</sup> and O5<sup>vii</sup> in adjacent chains. Despite the O1W...O1<sup>vi</sup> hydrogen bond noted in Table 4, the geometry at O1 is unfavorable for such an interaction and at best is a very weak interaction. The overall motif is a three-dimensional hydrogen-bonded network.

### Funding information

Funding for this research was provided by: National Science Foundation (grant Nos. CHE 1402744 and CHE 1707660 to AS).

### References

Table 4 Hydrogen-bond geometry (Å, °).				
<i>D</i> —H... <i>A</i>	<i>D</i> —H	H... <i>A</i>	<i>D</i> ... <i>A</i>	<i>D</i> —H... <i>A</i>
O4—H4O...O7 <sup>i</sup>	0.83 (3)	1.94 (3)	2.764 (2)	175 (3)
O6—H6O...O2 <sup>ii</sup>	0.83 (3)	1.96 (3)	2.793 (2)	173 (3)
O2'—H2'O...O1W	0.82 (3)	2.10 (3)	2.902 (2)	165 (3)
O3'—H3'O...O4 <sup>iii</sup>	0.84 (3)	1.96 (3)	2.7820 (19)	168 (2)
O4'—H4'O...O1W <sup>iv</sup>	0.84 (4)	2.17 (3)	2.9463 (19)	153 (3)
O6'—H6'O...O6 <sup>v</sup>	0.82 (4)	2.06 (4)	2.819 (2)	153 (3)
O1W—H1WA...O1 <sup>vi</sup>	0.86 (3)	2.58 (3)	3.224 (2)	133 (3)
O1W—H1WA...O5 <sup>vi</sup>	0.86 (3)	2.23 (3)	3.0838 (18)	170 (3)
O1W—H1WB...O5 <sup>vii</sup>	0.81 (4)	2.12 (4)	2.9303 (19)	177 (3)

Symmetry codes: (i)  $x - 1, y, z$ ; (ii)  $y, -x + y + 1, z + \frac{1}{6}$ ; (iii)  $x, y - 1, z$ ; (iv)  $x + 1, y, z$ ; (v)  $x - y + 1, x, z - \frac{1}{6}$ ; (vi)  $x - y, x - 1, z - \frac{1}{6}$ ; (vii)  $x - 1, y - 1, z$ .

A., Euell, C., Meredith, R., Carmichael, I. & Serianni, A. S. (2017). *NMR in Glycoscience and Glycotechnology*, p. 59. London: Royal Society of Chemistry.

Helenius, A. & Aeby, M. (2001). *Science*, **291**, 2364–2369.

Jeffrey, G. A., McMullan, R. K. & Takagi, S. (1977). *Acta Cryst. B33*, 728–737.

Kirby, A. J. (1983). In *The Anomeric Effect and Related Stereoelectronic Effects at Oxygen*, Vol. 15. Berlin: Springer-Verlag.

Krause, L., Herbst-Irmer, R., Sheldrick, G. M. & Stalke, D. (2015). *J. Appl. Cryst.* **48**, 3–10.

Macrae, C. F., Bruno, I. J., Chisholm, J. A., Edgington, P. R., McCabe, P., Pidcock, E., Rodriguez-Monge, L., Taylor, R., van de Streek, J. & Wood, P. A. (2008). *J. Appl. Cryst.* **41**, 466–470.

Nagae, M. & Yamaguchi, Y. (2012). *Int. J. Mol. Sci.* **13**, 8398–8429.

Parsons, S., Flack, H. D. & Wagner, T. (2013). *Acta Cryst. B69*, 249–259.

Satoh, T., Yamaguchi, T. & Kato, K. (2015). *Molecules*, **20**, 2475–2491.

Schmidt, R. R. & Michel, J. (1985). *J. Carbohydr. Chem.* **4**, 141–169.

Sheldrick, G. M. (2015a). *Acta Cryst. A71*, 3–8.

Sheldrick, G. M. (2015b). *Acta Cryst. C71*, 3–8.

Spek, A. L. (2009). *Acta Cryst. D65*, 148–155.

Thøgersen, H., Lemieux, R. U., Bock, K. & Meyer, B. (1982). *Can. J. Chem.* **60**, 44–57.

Turney, T., Zhang, W., Oliver, A. G. & Serianni, A. S. (2019). *Acta Cryst. C75*. Submitted.

Tvaroška, I. & Bleha, T. (1989). *Adv. Carbohydr. Chem. Biochem.* **47**, 45–123.

Westrip, S. P. (2010). *J. Appl. Cryst.* **43**, 920–925.

Zhang, W., Meredith, R., Pan, Q., Wang, X., Woods, R. J., Carmichael, I. & Serianni, A. S. (2019). *Biochemistry*, **58**, 546–560.

Zhang, W., Turney, T., Meredith, R., Pan, Q., Sernau, L., Wang, X., Hu, X., Woods, R. J., Carmichael, I. & Serianni, A. S. (2017). *J. Phys. Chem. B*, **121**, 3042–3058.

## supporting information

*Acta Cryst.* (2019). **C75** [https://doi.org/10.1107/S2053229619004728]

## Conformational analysis of the disaccharide methyl $\alpha$ -D-mannopyranosyl-(1 $\rightarrow$ 3)-2-O-acetyl- $\beta$ -D-mannopyranoside monohydrate

**Wenhui Zhang, Qingquan Wu, Allen G. Oliver and Anthony S. Serianni**

### Computing details

Data collection: *APEX3* (Bruker, 2015); cell refinement: *SAINT* (Bruker, 2015); data reduction: *SAINT* (Bruker, 2015); program(s) used to solve structure: *SHELXT2014* (Sheldrick, 2015a); program(s) used to refine structure: *SHELXL2018* (Sheldrick, 2015b); molecular graphics: *Mercury* (Macrae *et al.*, 2008); software used to prepare material for publication: *publCIF* (Westrip, 2010) and *PLATON* (Spek, 2009).

### Methyl $\alpha$ -D-mannopyranosyl-(1-3)-2-O-Acetyl- $\beta$ -D-mannopyranoside monohydrate

#### Crystal data

$C_{15}H_{26}O_{12}\cdot H_2O$   
 $M_r = 416.37$   
Hexagonal,  $P6_5$   
 $a = 7.8682 (3) \text{ \AA}$   
 $c = 52.555 (3) \text{ \AA}$   
 $V = 2817.7 (3) \text{ \AA}^3$   
 $Z = 6$   
 $F(000) = 1332$

$D_x = 1.472 \text{ Mg m}^{-3}$   
 $Cu K\alpha$  radiation,  $\lambda = 1.54184 \text{ \AA}$   
Cell parameters from 9714 reflections  
 $\theta = 6.5\text{--}72.2^\circ$   
 $\mu = 1.13 \text{ mm}^{-1}$   
 $T = 120 \text{ K}$   
Block, colourless  
 $0.30 \times 0.23 \times 0.14 \text{ mm}$

#### Data collection

Bruker APEXII  
diffractometer  
Radiation source: Incoatec micro-focus  
Detector resolution: 8.33 pixels  $\text{mm}^{-1}$   
combination of  $\omega$  and  $\varphi$ -scans  
Absorption correction: numerical  
(SADABS; Krause *et al.*, 2015)  
 $T_{\min} = 0.816$ ,  $T_{\max} = 0.907$

37134 measured reflections  
3719 independent reflections  
3719 reflections with  $I > 2\sigma(I)$   
 $R_{\text{int}} = 0.021$   
 $\theta_{\max} = 72.6^\circ$ ,  $\theta_{\min} = 5.1^\circ$   
 $h = -9 \rightarrow 9$   
 $k = -9 \rightarrow 9$   
 $l = -64 \rightarrow 64$

#### Refinement

Refinement on  $F^2$   
Least-squares matrix: full  
 $R[F^2 > 2\sigma(F^2)] = 0.022$   
 $wR(F^2) = 0.058$   
 $S = 1.06$   
3719 reflections  
287 parameters  
1 restraint  
Primary atom site location: dual

Secondary atom site location: difference Fourier  
map  
Hydrogen site location: mixed  
H atoms treated by a mixture of independent  
and constrained refinement  
 $w = 1/[\sigma^2(F_o^2) + (0.0341P)^2 + 0.5721P]$   
where  $P = (F_o^2 + 2F_c^2)/3$   
 $(\Delta/\sigma)_{\max} = 0.001$   
 $\Delta\rho_{\max} = 0.20 \text{ e \AA}^{-3}$   
 $\Delta\rho_{\min} = -0.16 \text{ e \AA}^{-3}$

Absolute structure: Flack  $x$  determined using  
 1835 quotients  $[(I+)-(I-)]/[(I+)+(I-)]$  (Parsons *et al.*, 2013)  
 Absolute structure parameter: 0.028 (14)

*Special details*

**Geometry.** All esds (except the esd in the dihedral angle between two l.s. planes) are estimated using the full covariance matrix. The cell esds are taken into account individually in the estimation of esds in distances, angles and torsion angles; correlations between esds in cell parameters are only used when they are defined by crystal symmetry. An approximate (isotropic) treatment of cell esds is used for estimating esds involving l.s. planes.

*Fractional atomic coordinates and isotropic or equivalent isotropic displacement parameters ( $\text{\AA}^2$ )*

	<i>x</i>	<i>y</i>	<i>z</i>	$U_{\text{iso}}^*/U_{\text{eq}}$
O1	1.05807 (18)	1.00809 (19)	0.54669 (3)	0.0230 (3)
O2	0.76178 (17)	0.62776 (18)	0.54504 (2)	0.0167 (2)
O4	0.31695 (19)	0.68238 (19)	0.50809 (2)	0.0177 (3)
H4O	0.216 (4)	0.636 (4)	0.5168 (5)	0.030 (7)*
O5	0.75643 (17)	0.97678 (18)	0.54738 (2)	0.0166 (3)
O6	0.3921 (3)	0.8446 (3)	0.57154 (3)	0.0380 (4)
H6O	0.338 (4)	0.879 (5)	0.5823 (6)	0.039 (8)*
O7	0.9678 (2)	0.5185 (2)	0.53482 (3)	0.0325 (3)
C1	0.8953 (2)	0.9597 (3)	0.53176 (3)	0.0173 (3)
H1	0.932708	1.050903	0.516908	0.021*
C2	0.8101 (2)	0.7488 (2)	0.52257 (3)	0.0157 (3)
H2	0.906976	0.734740	0.511761	0.019*
C3	0.6224 (3)	0.6899 (2)	0.50786 (3)	0.0144 (3)
H3	0.655673	0.773981	0.492323	0.017*
C4	0.4795 (2)	0.7205 (2)	0.52397 (3)	0.0142 (3)
H4	0.433840	0.628109	0.538762	0.017*
C5	0.5825 (2)	0.9338 (2)	0.53345 (3)	0.0152 (3)
H5	0.621069	1.023095	0.518385	0.018*
C6	0.4526 (3)	0.9744 (3)	0.55047 (3)	0.0191 (3)
H6A	0.525433	1.111930	0.556524	0.023*
H6B	0.336352	0.955685	0.540846	0.023*
C7	1.1834 (3)	1.2161 (3)	0.54980 (4)	0.0271 (4)
H7A	1.280757	1.241343	0.563074	0.041*
H7B	1.104304	1.275216	0.554727	0.041*
H7C	1.250786	1.273739	0.533717	0.041*
C8	0.8604 (2)	0.5337 (3)	0.54988 (4)	0.0182 (3)
C9	0.8169 (3)	0.4518 (3)	0.57627 (4)	0.0239 (4)
H9A	0.852907	0.349586	0.577821	0.036*
H9B	0.676564	0.395113	0.579779	0.036*
H9C	0.892892	0.556861	0.588507	0.036*
O1'	0.53187 (18)	0.48920 (18)	0.50014 (2)	0.0163 (2)
O2'	0.27523 (19)	0.22351 (19)	0.44429 (2)	0.0177 (3)
H2'O	0.172 (4)	0.119 (4)	0.4428 (5)	0.032 (7)*
O3'	0.27615 (19)	-0.08114 (18)	0.47211 (3)	0.0212 (3)
H3'O	0.301 (3)	-0.151 (4)	0.4816 (5)	0.018 (5)*

O4'	0.6920 (2)	0.05956 (19)	0.46951 (2)	0.0216 (3)
H4'O	0.753 (5)	0.048 (5)	0.4571 (7)	0.047 (8)*
O5'	0.66923 (17)	0.51175 (17)	0.46008 (2)	0.0148 (2)
O6'	0.8987 (2)	0.4274 (2)	0.42393 (3)	0.0251 (3)
H6'O	0.816 (5)	0.456 (5)	0.4197 (6)	0.044 (8)*
C1'	0.4947 (2)	0.4615 (2)	0.47384 (3)	0.0146 (3)
H1'	0.441294	0.546391	0.467925	0.017*
C2'	0.3387 (2)	0.2467 (2)	0.47017 (3)	0.0158 (3)
H2'	0.224819	0.214483	0.481598	0.019*
C3'	0.4230 (3)	0.1157 (2)	0.47688 (3)	0.0163 (3)
H3'	0.455995	0.130532	0.495416	0.020*
C4'	0.6097 (3)	0.1767 (2)	0.46164 (3)	0.0162 (3)
H4'	0.577373	0.155603	0.443093	0.019*
C5'	0.7577 (2)	0.3936 (2)	0.46646 (3)	0.0152 (3)
H5'	0.795964	0.412690	0.484833	0.018*
C6'	0.9407 (3)	0.4712 (3)	0.45016 (4)	0.0202 (4)
H6'A	1.019956	0.615329	0.452287	0.024*
H6'B	1.020419	0.413976	0.456212	0.024*
O1W	-0.1202 (2)	-0.1001 (2)	0.43620 (3)	0.0220 (3)
H1WA	-0.133 (4)	-0.130 (4)	0.4204 (7)	0.041 (8)*
H1WB	-0.174 (5)	-0.207 (5)	0.4430 (6)	0.043 (8)*

Atomic displacement parameters ( $\text{\AA}^2$ )

	$U^{11}$	$U^{22}$	$U^{33}$	$U^{12}$	$U^{13}$	$U^{23}$
O1	0.0166 (6)	0.0188 (6)	0.0343 (7)	0.0093 (5)	-0.0071 (5)	-0.0058 (5)
O2	0.0181 (6)	0.0186 (6)	0.0172 (6)	0.0120 (5)	0.0012 (5)	0.0010 (5)
O4	0.0141 (6)	0.0217 (6)	0.0157 (6)	0.0076 (5)	-0.0007 (5)	0.0009 (5)
O5	0.0170 (6)	0.0193 (6)	0.0161 (6)	0.0110 (5)	-0.0027 (5)	-0.0041 (5)
O6	0.0642 (11)	0.0549 (10)	0.0193 (7)	0.0481 (10)	0.0177 (7)	0.0105 (7)
O7	0.0292 (7)	0.0345 (8)	0.0446 (9)	0.0241 (7)	0.0147 (7)	0.0118 (7)
C1	0.0140 (7)	0.0173 (8)	0.0202 (8)	0.0075 (6)	0.0004 (6)	-0.0010 (6)
C2	0.0170 (8)	0.0160 (8)	0.0160 (8)	0.0098 (7)	0.0039 (6)	0.0012 (6)
C3	0.0172 (8)	0.0127 (7)	0.0126 (7)	0.0070 (6)	0.0015 (6)	-0.0003 (6)
C4	0.0146 (7)	0.0161 (8)	0.0115 (7)	0.0074 (6)	-0.0006 (6)	0.0002 (6)
C5	0.0156 (7)	0.0165 (8)	0.0154 (8)	0.0095 (6)	-0.0018 (6)	-0.0004 (6)
C6	0.0225 (9)	0.0220 (8)	0.0175 (8)	0.0146 (7)	0.0003 (6)	-0.0027 (7)
C7	0.0165 (9)	0.0195 (9)	0.0417 (12)	0.0063 (7)	-0.0015 (8)	-0.0094 (8)
C8	0.0110 (7)	0.0158 (8)	0.0270 (9)	0.0061 (6)	-0.0024 (6)	-0.0032 (7)
C9	0.0276 (9)	0.0255 (9)	0.0241 (10)	0.0174 (8)	-0.0072 (8)	-0.0029 (7)
O1'	0.0219 (6)	0.0141 (6)	0.0119 (6)	0.0083 (5)	0.0007 (5)	-0.0017 (4)
O2'	0.0167 (6)	0.0173 (6)	0.0134 (6)	0.0044 (5)	-0.0020 (4)	0.0017 (4)
O3'	0.0218 (6)	0.0135 (6)	0.0222 (6)	0.0043 (5)	-0.0049 (5)	0.0018 (5)
O4'	0.0291 (7)	0.0228 (6)	0.0201 (6)	0.0183 (6)	0.0052 (5)	0.0039 (5)
O5'	0.0168 (6)	0.0134 (5)	0.0135 (5)	0.0070 (5)	0.0026 (4)	0.0007 (4)
O6'	0.0249 (7)	0.0293 (7)	0.0202 (7)	0.0130 (6)	0.0075 (5)	-0.0021 (5)
C1'	0.0165 (8)	0.0151 (7)	0.0121 (7)	0.0079 (6)	0.0021 (6)	0.0007 (6)
C2'	0.0151 (8)	0.0173 (8)	0.0119 (7)	0.0059 (7)	0.0011 (6)	0.0008 (6)

C3'	0.0173 (8)	0.0131 (8)	0.0147 (8)	0.0048 (7)	-0.0008 (6)	-0.0002 (6)
C4'	0.0203 (8)	0.0150 (8)	0.0142 (7)	0.0096 (7)	-0.0004 (6)	-0.0006 (6)
C5'	0.0172 (8)	0.0156 (8)	0.0139 (8)	0.0090 (7)	-0.0014 (6)	-0.0024 (6)
C6'	0.0175 (8)	0.0195 (8)	0.0219 (9)	0.0081 (7)	0.0018 (7)	-0.0013 (7)
O1W	0.0264 (7)	0.0186 (7)	0.0197 (7)	0.0102 (6)	-0.0002 (5)	0.0010 (5)

Geometric parameters ( $\text{\AA}$ ,  $^\circ$ )

O1—C1	1.383 (2)	C9—H9A	0.9800
O1—C7	1.437 (2)	C9—H9B	0.9800
O2—C8	1.337 (2)	C9—H9C	0.9800
O2—C2	1.444 (2)	O1'—C1'	1.407 (2)
O4—C4	1.428 (2)	O2'—C2'	1.429 (2)
O4—H4O	0.83 (3)	O2'—H2'O	0.82 (3)
O5—C1	1.426 (2)	O3'—C3'	1.417 (2)
O5—C5	1.435 (2)	O3'—H3'O	0.84 (3)
O6—C6	1.417 (2)	O4'—C4'	1.428 (2)
O6—H6O	0.83 (3)	O4'—H4'O	0.84 (4)
O7—C8	1.207 (2)	O5'—C1'	1.422 (2)
C1—C2	1.524 (2)	O5'—C5'	1.452 (2)
C1—H1	1.0000	O6'—C6'	1.419 (2)
C2—C3	1.520 (2)	O6'—H6'O	0.82 (4)
C2—H2	1.0000	C1'—C2'	1.525 (2)
C3—O1'	1.429 (2)	C1'—H1'	1.0000
C3—C4	1.520 (2)	C2'—C3'	1.521 (2)
C3—H3	1.0000	C2'—H2'	1.0000
C4—C5	1.537 (2)	C3'—C4'	1.524 (2)
C4—H4	1.0000	C3'—H3'	1.0000
C5—C6	1.508 (2)	C4'—C5'	1.531 (2)
C5—H5	1.0000	C4'—H4'	1.0000
C6—H6A	0.9900	C5'—C6'	1.517 (2)
C6—H6B	0.9900	C5'—H5'	1.0000
C7—H7A	0.9800	C6'—H6'A	0.9900
C7—H7B	0.9800	C6'—H6'B	0.9900
C7—H7C	0.9800	O1W—H1WA	0.86 (3)
C8—C9	1.495 (3)	O1W—H1WB	0.81 (4)
C1—O1—C7	113.08 (14)	C8—C9—H9A	109.5
C8—O2—C2	119.09 (13)	C8—C9—H9B	109.5
C4—O4—H4O	109.2 (18)	H9A—C9—H9B	109.5
C1—O5—C5	111.68 (12)	C8—C9—H9C	109.5
C6—O6—H6O	110 (2)	H9A—C9—H9C	109.5
O1—C1—O5	107.16 (14)	H9B—C9—H9C	109.5
O1—C1—C2	108.81 (14)	C1'—O1'—C3	113.60 (13)
O5—C1—C2	110.15 (14)	C2'—O2'—H2'O	109 (2)
O1—C1—H1	110.2	C3'—O3'—H3'O	106.5 (17)
O5—C1—H1	110.2	C4'—O4'—H4'O	108 (2)
C2—C1—H1	110.2	C1'—O5'—C5'	114.20 (12)

O2—C2—C3	108.63 (13)	C6'—O6'—H6'O	108 (2)
O2—C2—C1	106.63 (13)	O1'—C1'—O5'	111.09 (13)
C3—C2—C1	108.94 (14)	O1'—C1'—C2'	106.59 (13)
O2—C2—H2	110.8	O5'—C1'—C2'	111.97 (13)
C3—C2—H2	110.8	O1'—C1'—H1'	109.0
C1—C2—H2	110.8	O5'—C1'—H1'	109.0
O1'—C3—C4	109.51 (14)	C2'—C1'—H1'	109.0
O1'—C3—C2	110.66 (13)	O2'—C2'—C3'	112.14 (14)
C4—C3—C2	110.58 (13)	O2'—C2'—C1'	107.36 (13)
O1'—C3—H3	108.7	C3'—C2'—C1'	109.84 (14)
C4—C3—H3	108.7	O2'—C2'—H2'	109.1
C2—C3—H3	108.7	C3'—C2'—H2'	109.1
O4—C4—C3	107.27 (13)	C1'—C2'—H2'	109.1
O4—C4—C5	110.30 (13)	O3'—C3'—C2'	107.83 (14)
C3—C4—C5	108.98 (13)	O3'—C3'—C4'	112.47 (14)
O4—C4—H4	110.1	C2'—C3'—C4'	110.07 (14)
C3—C4—H4	110.1	O3'—C3'—H3'	108.8
C5—C4—H4	110.1	C2'—C3'—H3'	108.8
O5—C5—C6	108.35 (14)	C4'—C3'—H3'	108.8
O5—C5—C4	110.08 (13)	O4'—C4'—C3'	108.75 (14)
C6—C5—C4	112.36 (14)	O4'—C4'—C5'	109.48 (14)
O5—C5—H5	108.7	C3'—C4'—C5'	109.90 (14)
C6—C5—H5	108.7	O4'—C4'—H4'	109.6
C4—C5—H5	108.7	C3'—C4'—H4'	109.6
O6—C6—C5	109.25 (14)	C5'—C4'—H4'	109.6
O6—C6—H6A	109.8	O5'—C5'—C6'	105.90 (14)
C5—C6—H6A	109.8	O5'—C5'—C4'	109.51 (14)
O6—C6—H6B	109.8	C6'—C5'—C4'	113.28 (14)
C5—C6—H6B	109.8	O5'—C5'—H5'	109.4
H6A—C6—H6B	108.3	C6'—C5'—H5'	109.4
O1—C7—H7A	109.5	C4'—C5'—H5'	109.4
O1—C7—H7B	109.5	O6'—C6'—C5'	113.09 (15)
H7A—C7—H7B	109.5	O6'—C6'—H6'A	109.0
O1—C7—H7C	109.5	C5'—C6'—H6'A	109.0
H7A—C7—H7C	109.5	O6'—C6'—H6'B	109.0
H7B—C7—H7C	109.5	C5'—C6'—H6'B	109.0
O7—C8—O2	123.98 (18)	H6'A—C6'—H6'B	107.8
O7—C8—C9	125.89 (17)	H1WA—O1W—H1WB	102 (3)
O2—C8—C9	110.13 (15)		
C7—O1—C1—O5	-79.07 (18)	C2—O2—C8—C9	168.49 (15)
C7—O1—C1—C2	161.85 (15)	C4—C3—O1'—C1'	112.13 (15)
C5—O5—C1—O1	178.65 (13)	C2—C3—O1'—C1'	-125.72 (15)
C5—O5—C1—C2	-63.13 (18)	C3—O1'—C1'—O5'	77.51 (16)
C8—O2—C2—C3	128.63 (15)	C3—O1'—C1'—C2'	-160.26 (13)
C8—O2—C2—C1	-114.09 (16)	C5'—O5'—C1'—O1'	61.63 (17)
O1—C1—C2—O2	58.60 (17)	C5'—O5'—C1'—C2'	-57.43 (18)
O5—C1—C2—O2	-58.59 (17)	O1'—C1'—C2'—O2'	170.46 (13)

O1—C1—C2—C3	175.67 (14)	O5'—C1'—C2'—O2'	−67.87 (17)
O5—C1—C2—C3	58.48 (18)	O1'—C1'—C2'—C3'	−67.36 (16)
O2—C2—C3—O1'	−60.93 (16)	O5'—C1'—C2'—C3'	54.31 (18)
C1—C2—C3—O1'	−176.72 (13)	O2'—C2'—C3'—O3'	−58.14 (17)
O2—C2—C3—C4	60.60 (17)	C1'—C2'—C3'—O3'	−177.43 (13)
C1—C2—C3—C4	−55.19 (17)	O2'—C2'—C3'—C4'	64.88 (18)
O1'—C3—C4—O4	−63.88 (16)	C1'—C2'—C3'—C4'	−54.41 (18)
C2—C3—C4—O4	173.92 (13)	O3'—C3'—C4'—O4'	−63.40 (18)
O1'—C3—C4—C5	176.70 (13)	C2'—C3'—C4'—O4'	176.35 (13)
C2—C3—C4—C5	54.50 (17)	O3'—C3'—C4'—C5'	176.78 (13)
C1—O5—C5—C6	−174.48 (14)	C2'—C3'—C4'—C5'	56.52 (18)
C1—O5—C5—C4	62.30 (17)	C1'—O5'—C5'—C6'	−179.33 (14)
O4—C4—C5—O5	−174.52 (13)	C1'—O5'—C5'—C4'	58.19 (17)
C3—C4—C5—O5	−57.00 (17)	O4'—C4'—C5'—O5'	−176.17 (13)
O4—C4—C5—C6	64.63 (18)	C3'—C4'—C5'—O5'	−56.79 (18)
C3—C4—C5—C6	−177.85 (14)	O4'—C4'—C5'—C6'	65.87 (19)
O5—C5—C6—O6	−63.86 (19)	C3'—C4'—C5'—C6'	−174.75 (15)
C4—C5—C6—O6	58.0 (2)	O5'—C5'—C6'—O6'	−69.90 (18)
C2—O2—C8—O7	−11.7 (3)	C4'—C5'—C6'—O6'	50.1 (2)

Hydrogen-bond geometry ( $\text{\AA}$ ,  $^\circ$ )

$D—\text{H}\cdots A$	$D—\text{H}$	$\text{H}\cdots A$	$D\cdots A$	$D—\text{H}\cdots A$
O4—H4O $\cdots$ O7 <sup>i</sup>	0.83 (3)	1.94 (3)	2.764 (2)	175 (3)
O6—H6O $\cdots$ O2 <sup>ii</sup>	0.83 (3)	1.96 (3)	2.793 (2)	173 (3)
O2'—H2'O $\cdots$ O1W	0.82 (3)	2.10 (3)	2.902 (2)	165 (3)
O3'—H3'O $\cdots$ O4 <sup>iii</sup>	0.84 (3)	1.96 (3)	2.7820 (19)	168 (2)
O4'—H4'O $\cdots$ O1W <sup>iv</sup>	0.84 (4)	2.17 (3)	2.9463 (19)	153 (3)
O6'—H6'O $\cdots$ O6 <sup>v</sup>	0.82 (4)	2.06 (4)	2.819 (2)	153 (3)
O1W—H1WA $\cdots$ O1 <sup>vi</sup>	0.86 (3)	2.58 (3)	3.224 (2)	133 (3)
O1W—H1WA $\cdots$ O5 <sup>vi</sup>	0.86 (3)	2.23 (3)	3.0838 (18)	170 (3)
O1W—H1WB $\cdots$ O5 <sup>vii</sup>	0.81 (4)	2.12 (4)	2.9303 (19)	177 (3)

Symmetry codes: (i)  $x-1, y, z$ ; (ii)  $y, -x+y+1, z+1/6$ ; (iii)  $x, y-1, z$ ; (iv)  $x+1, y, z$ ; (v)  $x-y+1, x, z-1/6$ ; (vi)  $x-y, x-1, z-1/6$ ; (vii)  $x-1, y-1, z$ .